

# Offline AI-assisted fundus imaging for preliminary screening of childhood glaucoma

Sirisha Senthil, MS,<sup>a</sup> Divya Parthasarathy Rao, MS,<sup>b</sup> Shreya Bhandary, M Optom,<sup>c</sup> Rashmi Krishnamurthy, MD,<sup>a</sup> and Kalpa Negiloni, PhD<sup>c</sup>

<b>PURPOSE</b>	To evaluate the feasibility and performance of AI-assisted portable fundus photography in children with glaucoma.
<b>METHODS</b>	This case series describes the use of smartphone-based fundus imaging with integrated off-line glaucoma artificial intelligence (AI) in children ( $\leq 18$ years) with various types of glaucoma who were evaluated at a tertiary eye care center, and compares AI-derived referral recommendations with presence or absence of structural optic nerve changes determined on clinical evaluation.
<b>RESULTS</b>	AI-assisted fundus photography and clinical evaluation were completed for 21 children. For vertical cup:disk ratio, the 95% limits of agreement between AI image analysis and clinical assessment on Bland-Altman analysis were $-0.15$ to $+0.23$ . The AI output recommended referral for 7 of 8 children who had structural optic nerve changes on clinical examination and did not recommend referral for any of the children without such optic nerve changes.
<b>CONCLUSIONS</b>	AI-assisted smartphone-based fundus imaging may help identify cases of pediatric glaucoma exhibiting structural optic nerve changes. (J AAPOS 2026; ■:104755)



Pediatric glaucoma is a rare but potentially sight-threatening condition, with an incidence of approximately 2.29 per 100,000 individuals  $< 20$  years of age.<sup>1</sup> It includes primary congenital glaucoma (PCG), juvenile open-angle glaucoma, and secondary glaucomas associated with ocular or systemic disorders. If untreated, it can cause permanent visual impairment and blindness. Diagnosis often requires examination under anesthesia in young children, and management is primarily surgical, unlike adult glaucoma, where medications are usually first line of treatment.<sup>2</sup>

Artificial intelligence (AI) offers a promising tool to support early detection and monitoring of glaucoma in children. AI-assisted fundus imaging may provide rapid, objective assessment of optic nerve changes, which can improve referral accuracy and assist clinicians, particularly in settings with limited access to pediatric glaucoma specialists. This case se-

ries evaluates the feasibility and performance of AI-assisted portable fundus photography in children, comparing AI-based referral decisions with clinical diagnosis.

## Subjects and Methods

This prospective study included 21 consecutive pediatric patients ( $\leq 18$  years) seen at L V Prasad Eye Institute from September 2022 to November 2022. Approval of the L V Prasad Eye Institute Institutional Review Board, and parental consent was obtained for use of clinical images. Anonymized clinical data collected during routine care were analyzed.

All patients underwent a comprehensive ophthalmic examination, including best-corrected visual acuity, intraocular pressure (IOP) assessment (Perkins tonometer, Haag-Streit, Switzerland), central corneal thickness measurement, slit-lamp biomicroscopy, gonioscopy, and fundus evaluation by two glaucoma consultants (SIR, RKM). Additional tests included visual field analysis, anterior segment photography (PSL-D20, Remidio Innovative Solutions Pvt Ltd, Bengaluru, India), and topography when indicated. Optic disk appearance was documented using portable fundus photography (FOP NM-10, Remidio Innovative Solutions). Images were captured without dilation, and if quality remained insufficient after two additional attempts, the same procedure was repeated following dilation. The images were analyzed using an offline AI-based glaucoma screening algorithm (MediosHI Glaucoma AI, Remidio Innovative Solutions). The Medios Glaucoma AI system consists of two components: (1) a cup-disk segmentation model that outputs the vertical cup:disk ratio (vCDR), and (2) a binary classification

Author affiliations: <sup>a</sup>VST Center for Glaucoma Care, LV Prasad Eye Institute, Hyderabad, India; <sup>b</sup>Remidio Innovative Solutions Pvt Ltd, Glen Allen, Virginia; <sup>c</sup>Remidio Innovative Solutions Pvt Ltd, Bengaluru, Karnataka, India

Conflicts of Interest: Divya Parthasarathy Rao, Shreya Bhandary and Kalpa Negiloni are employees of Remidio Innovative Solutions. Remidio Innovative Solutions, Glen Allen, VA, United States, is a wholly owned subsidiary of Remidio Innovative Solutions Pvt Ltd, Bengaluru, Karnataka, India.

Submitted August 2, 2025.

Revision accepted October 20, 2025.

Correspondence: Dr Sirisha Senthil, L V Prasad Eye Institute, Dr. Kallam Anji Reddy Campus, Banjara Hills, Hyderabad 500 034, India (email: [sirishasenthil@lvpei.org](mailto:sirishasenthil@lvpei.org)).  
J AAPOS 2026; ■:104755.

© 2026 by the American Association for Pediatric Ophthalmology and Strabismus.

1091-8531/836.00

<https://doi.org/10.1016/j.jaaapos.2026.104755>

model that categorizes images into “referable glaucoma” versus suspects/normal eyes, trained using datasets that incorporate optic disk and retinal nerve fiber layer (RNFL) features beyond vCDR. The development of the glaucoma AI model has been previously described and externally validated in prospective studies conducted across diverse clinical and community eye care settings.<sup>3,4</sup>

### Statistical Analysis

AI-derived and clinician-measured vCDR were assessed using Pearson correlation and Bland-Altman analysis. AI referral output was compared with clinical diagnosis for concordance. Analyses used SPSS Statistics version 20 (IBM Corp, Armonk, NY), with  $P < 0.05$  considered significant. Three authors (DRP, SB, KN) are employees of the device manufacturer and provided technical support for device use; however, they were not involved in patient recruitment, image grading, or data analysis. All analyses were performed independently to minimize potential bias.

### Results

Fundus imaging was performed on 21 children (13 males; mean participant age, 12.6 years). Average visual acuity (worse eye) was 0.72 logMAR (range, 0–3.0 logMAR), with 13 patients (62%) having  $\geq 20/40$  in at least one eye. In all but 2 cases, images were captured undilated. Four eyes required a second or third attempt (undilated pupils) to achieve adequate image quality.

Correlation analysis between AI-derived and clinically measured vCDR showed strong correlation, with Pearson coefficients of 0.93 for left eyes and 0.95 for right eyes ( $P < 0.00001$ ; Figure 1A). The Bland-Altman plot in Figure 1B shows a mean bias of 0.04 (95% confidence limits,  $-0.15$  to  $+0.23$ ).

The AI software output referral recommendation for each case was also recorded to evaluate its concordance with clinical diagnosis. In the primary congenital glaucoma group, the glaucoma AI accurately identified all 3 cases of referable glaucoma with structural changes, consistent with the clinical specialist diagnosis. The remaining 4 eyes, which had no structural changes of the optic nerve, were not flagged for referral. Among the secondary glaucoma cases, the AI correctly identified 4 of 5 glaucoma cases with structural optic nerve changes for referral, missing only a single case involving a patient with Sturge-Weber syndrome with subtle structural changes of inferior rim thinning in one eye. Additionally, eyes without structural changes were correctly identified as not exhibiting glaucomatous optic nerve changes by the AI. The clinical details of the entire cohort and AI outputs are summarized in Table S1 (Supplement 1, available at [jaapos.org](http://jaapos.org)), with class activation maps highlighting optic disk structural changes associated with glaucomatous

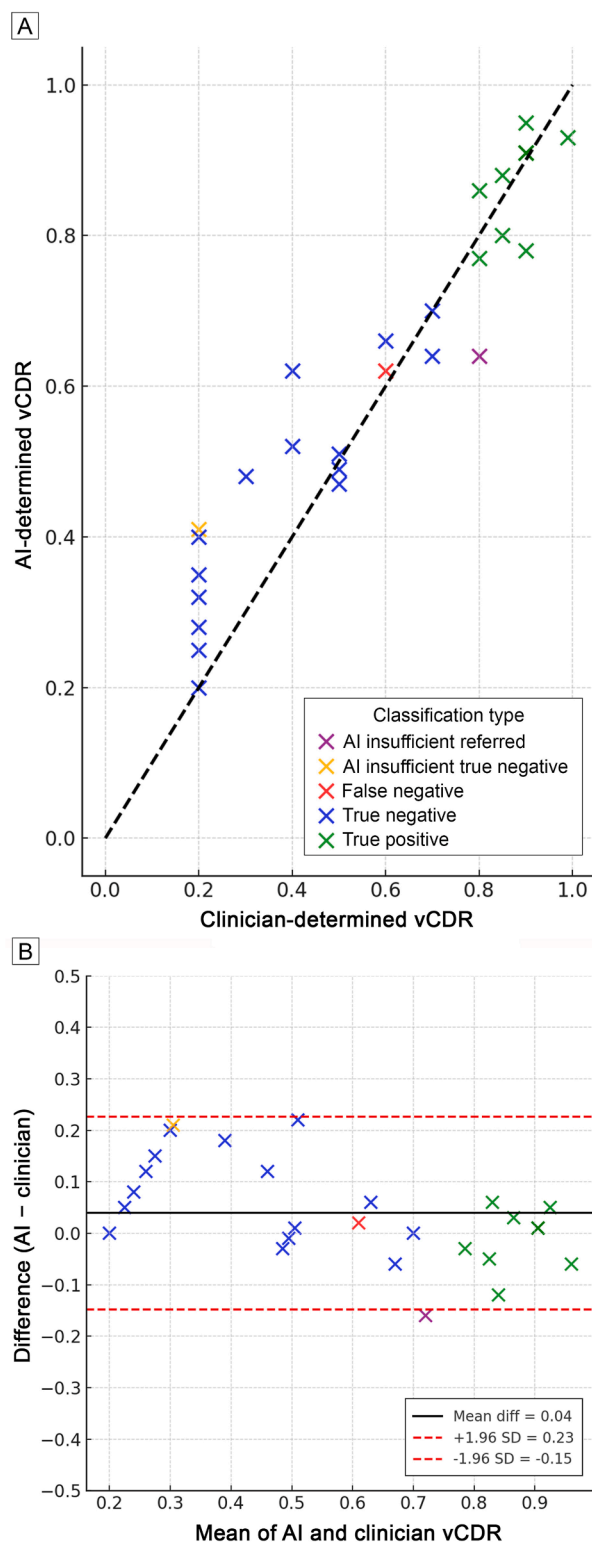


**FIG 1.** A, Scatterplot comparing AI-determined versus clinician-determined vertical cup:disc ratio (vCDR), color-coded also with regard to concordance between referral recommendation and clinical determination of structural optic nerve changes (true positives, true negatives and false negatives). B, Bland-Altman plot illustrating the agreement between AI and clinician vCDR values.

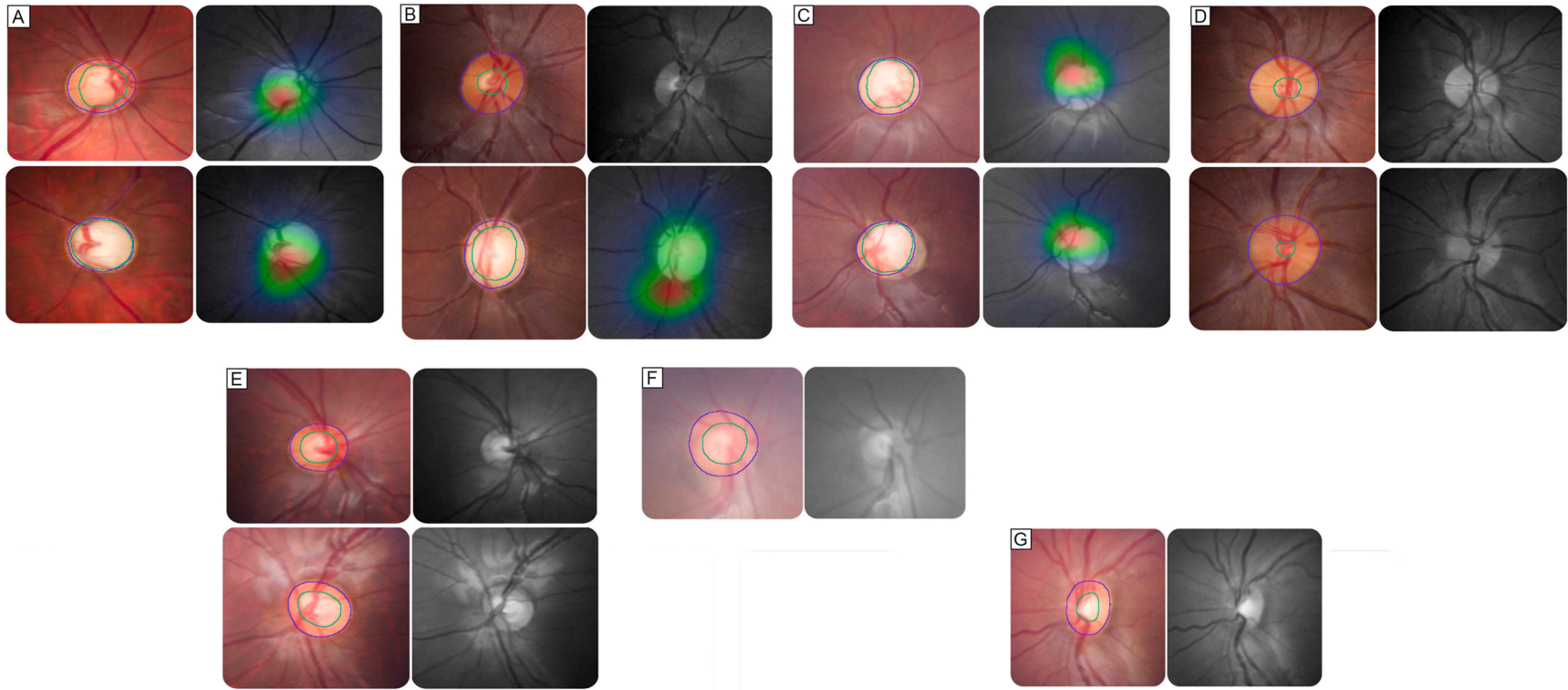


**FIG 2.** Primary congenital glaucoma AI output with class activation maps for referral-warranted findings, with warm colors highlighting lesion areas that the AI identified as glaucomatous changes. Top row of each set is right eye; bottom row, left eye. Cases with referable glaucoma (eye [AI-determined vCDR right/left]): A (both eyes [0.8/0.95]), B (left eye only [0.4/0.78]), C (both eyes 0.86/0.91). See [Table S1](#) for patient details. vCDR, vertical cup:disk ratio.

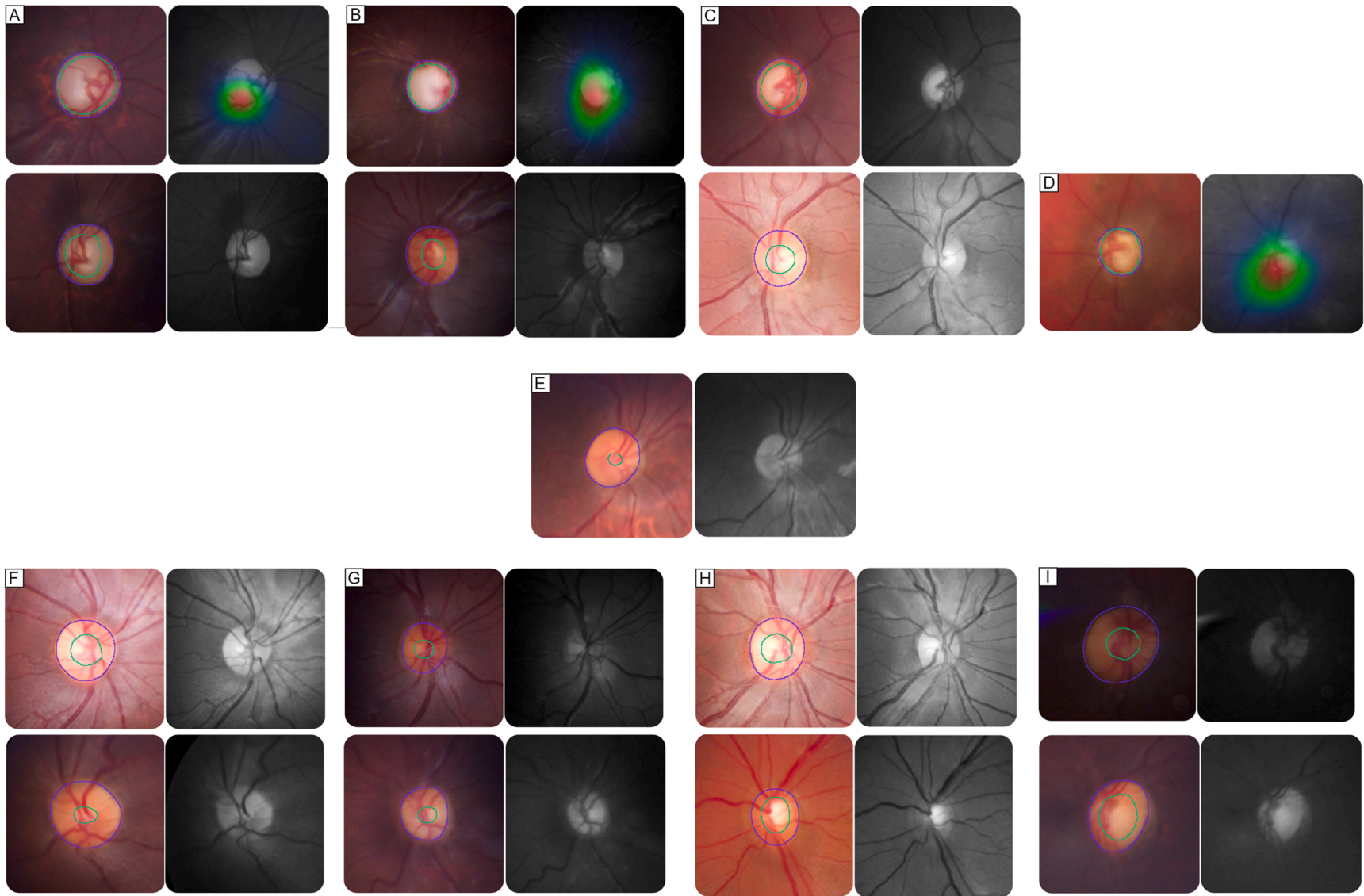


**FIG 3.** Secondary glaucoma AI output with class activation maps for referral-warranted findings, with warm colors highlighting lesion areas that the AI identified as glaucomatous changes. Cases with referable glaucoma (eye [AI-determined vCDR right/left]): A (both eyes [0.88/0.7]), B (right eye only [0.91/0.48]), D (left eye only [0.93]). The right eye of patient 10 (C) was suspect, with a high vCDR (0.77). Both eyes of patient 16 were referred because of insufficient quality. See [Table S1](#) for patient details. vCDR, vertical cup:disk ratio.

damage shown in [Figures 2](#) and [3](#) for both primary and secondary cases.

## Discussion

This case series highlights the potential use of an offline AI-based screening tool for pediatric glaucoma, a condition with diverse and complex presentations. AI technology could enhance early detection, triage, and clinical decision making, especially where visual field testing is unreliable and normative optical coherence tomography (OCT) data are limited.<sup>2</sup>

AI-assisted portable fundus imaging was technically feasible and demonstrated strong concordance with expert diagnosis in eyes with structural optic nerve damage. The AI effectively detected classic glaucomatous changes (increased cup:disc ratio, rim thinning, notches, disc asymmetry). Performance was strongest in PCG, where optic nerve cupping patterns resemble those in adult glaucoma. Secondary glaucomas were also well detected, although a single Sturge-Weber case with early optic nerve changes was missed, indicating the need for algorithm refinement for early or atypical changes.

Portable AI-enabled fundus cameras proved practical in children, who often cannot cooperate for conventional testing, and may also be valuable in settings without advanced imaging (eg, OCT). AI enables standardized, repeatable optic disk assessments, supports early detection and referral prioritization,<sup>5</sup> and reduces reliance on examinations under anesthesia. Documenting optic disk changes longitudinally is critical, as progression can occur despite intervention; alternative progression markers in children include axial length changes, refractive error shifts, corneal parameters, and IOP variation.

Current AI limitations provide opportunities for enhancement, especially in recognizing early or atypical disc changes seen in trauma- or steroid-related or syndromic glaucomas. Future models could incorporate multimodal

data (anterior segment imaging, IOP, axial length, refraction, visual fields) to improve diagnostic accuracy.<sup>6,7</sup>

Despite challenges in pediatric imaging, the AI successfully flagged the abnormal optic nerves in our cohort, including discs with rim thinning and pallor, even when image quality was suboptimal; most pupils were imaged undilated. The small sample size, lack of controls, and use of an AI trained on adult datasets limit the generalizability of our results, but our findings are nonetheless encouraging. AI missed 1 case with atypical glaucomatous optic disk morphology, highlighting the need for more varied training datasets. Future studies could incorporate normative data of pediatric eyes that could be used to train the AI model and also plan independent external validation on larger cohorts.

## References

1. Aponte EP, Diehl N, Mohny BG. Incidence and clinical characteristics of childhood glaucoma: a population-based study. *Arch Ophthalmol* 2010;128:478-82.
2. Pirlich N, Grehn F, Mohnke K, et al. Anaesthetic protocol for paediatric glaucoma examinations: the prospective EyeBIS study protocol. *BMJ Open* 2021;11:e045906.
3. Shroff S, Rao DP, Savoy FM, et al. Agreement of a novel artificial intelligence software with optical coherence tomography and manual grading of the optic disc in glaucoma. *J Glaucoma* 2023;32:280-86.
4. Upadhyaya S, Rao DP, Kavitha S, et al. Diagnostic performance of the offline Medios artificial intelligence for glaucoma detection in a rural tele-ophthalmology setting. *Ophthalmol Glaucoma* 2025;8:28-36.
5. Bragança CP, Torres JM, Soares CPDA, et al. Detection of glaucoma on fundus images using deep learning on a new image set obtained with a smartphone and handheld ophthalmoscope. *Healthcare (Basel)* 2022; 10:2345.
6. Sihota R, Angmo D, Ramaswamy D, et al. Simplifying “target” intraocular pressure for different stages of primary open-angle glaucoma and primary angle-closure glaucoma. *Indian J Ophthalmol* 2018;66: 495-505.
7. Medeiros FA, Sample PA, Zangwill LM, et al. Corneal thickness as a risk factor for visual field loss in patients with preperimetric glaucomatous optic neuropathy. *Am J Ophthalmol* 2003;136:805-13.